Journal of Catalysis **189,** 431–437 (2000)
doi:10.1006/jcat.1999.2715, available online at http://www.idealibrary.com on IDEAL®

Modifications of Surface Properties of a H_2-treated RuS_2/SiO_2 Catalyst: A Parallel between Low-Temperature CO FTIR Spectroscopy and Model Reactions

Gilles Berhault,* Françoise Maugé,†,[1] Jean-Claude Lavalley,† Michel Lacroix,* and Michèle Breysse‡

*Institut de Recherches sur la Catalyse, 2 Avenue Albert Einstein, 69626 Villeurbanne Cedex, France; †Laboratoire Catalyse et Spectrochimie, ISMRA-Université, 6 Boulevard du Maréchal Juin, 14050 Caen Cedex, France; and ‡Laboratoire de Réactivité de Surface, Université P. et M. Curie, 4 Place Jussieu, Casier 178, 75252 Paris Cedex 05, France

Received July 2, 1999; revised September 1, 1999; accepted September 23, 1999

A silica-supported ruthenium sulfide catalyst was progressively reduced by hydrogen at increasing temperatures (423–673 K). The resulting modification of the surface properties was characterized by low-temperature CO adsorption FTIR spectroscopy and by test reactions such as CH_3SH condensation and 1-butene hydrogenation. On the nonreduced catalyst, CO adsorption spectra showed the presence of bands, indicating various CO forms on Ru sites in a sulfur-rich environment. When sulfur was progressively removed from the ruthenium sulfide phase, the number of coordinatively unsaturated Ru sites increased with the simultaneous formation of metallic Ru microdomains. A comparison of measurements of adsorption and catalytic activity showed that a rich sulfur environment was needed for the condensation of CH_3SH to CH_3SCH_3, a reaction that required acidic sites, while butene hydrogenation required highly depleted Ru sites. These results show that, upon reduction, RuS_2 became less acidic and increasingly more metallic.

INTRODUCTION

Extensive studies dealt with the characterization of the active sites of transition metal sulfide catalysts. It was shown that the formation of coordinatively unsaturated sites (CUS) (e.g., sulfur vacancies) (1, 2) plays an essential role in most reactions involved in hydrotreating processes, i.e., hydrodesulfurization, hydrodenitrogenation, and aromatics hydrogenation. The chemisorption of the unsaturated hydrocarbons or S- and N-containing molecules generally proceeds by electron donation to these vacant sites (3, 4). Accordingly, these CUS are considered to be a Lewis-type center interacting with electron-donating organic substrates. In addition to these organic molecules, H_2 and H_2S can become heterolytically dissociated on transition metal sulfide (TMS) surfaces, giving rise to the formation of SH groups. Thus, TMS catalysts possess several types of sites, i.e., CUS, SH groups, and sulfur anions, the relative proportions of which depend on the experimental conditions, temperature, or composition of the reducing atmosphere, i.e., H_2 or H_2S partial pressure. Thus, the characterization of these sites should be carried out *in situ* using physico–chemical techniques or model molecule reactions; it is essential to relate the catalytic properties to surface characterization for similar surface states. Several authors showed that the creation of various kinds of sites is achieved by progressive reductive hydrogen treatment (5–9). The properties of these sites as a function of the S/Me ratio were studied at temperatures lower than those at which the hydrogen treatments were carried out. This methodology was recently applied to study Brønsted and Lewis acidity of a model silica-supported ruthenium sulfide catalyst. Different probe molecules, namely, pyridine and 2,6-dimethylpyridine, were investigated by means of infrared adsorption measurements (10). Lewis acidity, characterized by pyridine adsorption, was maximum for an elimination of 20% of the initial sulfur content, although the structure of the pyrite RuS_2 phase was stable up to 45%. It was expected that the maximum of the number of Lewis sites would also be reached for this same degree of desulfurization. This discrepancy suggests that not only the number but also the strength of the Lewis acid sites were modified in such a way that highly depleted Ru sites were unable to chemisorb pyridine.

The aim of this study is to describe in detail the various sites formed during these reductive steps and to correlate these data to catalytic activity determined from a model hydrogenation reaction such as 1-butene hydrogenation. This reaction can be studied at 273 K, a temperature sufficiently low to prevent modification of the surface states induced by hydrogen treatment at higher temperatures. Low-temperature CO FTIR spectroscopy was utilized to characterize the variation in the nature and number of the surface sites of the RuS_x system and, in particular, the

[1] To whom all correspondence should be addressed. Fax: (+33) (0)2 31 45 28 22. E-mail: Francoise.Mauge@ismra.fr.

0021-9517/00 $35.00

formation of a metallic phase. CO is one of the most widely used probe molecules, and its interaction with the surface can be described according to the model proposed by Blyholder (11). The CO stretching frequency provides informative data about the oxidation state and the coordination number of the adsorbing sites (12–14). Because CO reacts with metallic Ru particles, leading to an increase in the metal dispersion and to the appearance of some ionic Ru sites (15–19), the adsorption experiments were performed preferably at low temperature (20, 21). The data will be compared to previous results which concern the characterization of solid acidity using nitrogen-containing probes and the CH_3SH condensation reaction (9, 10).

EXPERIMENTAL

Catalyst Preparation

The silica-supported RuS_2/SiO_2 was prepared using the pore-filling method. The silica support was a high surface area Grace Davison 432 (300 m^2/g BET area; pore volume 0.5 cm^3/g) which contained about 1500 ppm of alumina as impurities. The carrier was dried overnight at 383 K prior to impregnation with aqueous solutions of $RuCl_3$, xH_2O (Johnson Matthey). The impregnated silica was dried at 383 K and sulfided at 673 K in a 15%H_2S–85%N_2 atmosphere to avoid the formation of an intermediate metallic phase that is difficult to sulfide (22). After this activation procedure, the solids were cooled to room temperature in a sulfur atmosphere, flushed with an oxygen-free nitrogen flow, and stored in sealed bottles. The Ru loading was 7.5 wt%.

Catalyst Reduction and 1-Butene Hydrogenation

These experiments were performed *in situ* in the same flow microreactor. The unit was connected to a gas chromatograph equipped with two parallel detectors, a flame photometric detector (FPD) and a flame ionization detector (FID) to detect H_2S and the hydrocarbons, respectively.

The catalyst was loaded into the reactor and flushed under nitrogen for 15 min at room temperature (RT) and then put into contact with a 100 cm^3 min^{-1} hydrogen flow. Catalyst reduction was carried out by heating the reactor to the desired reduction temperature (T_r) using a heating rate of 2 K min^{-1} and left under isothermal conditions for 2 h. The amount of H_2S released by the solid was quantified by calibrating the FPD detector with a known concentration of H_2S (573 ppm) diluted in hydrogen. Gas samplings were taken every 2 min for analysis. The degree of reduction, α, was defined by the ratio of the amount of H_2S eliminated from the solid to the total sulfur content.

After this *in situ* reduction, hydrogen was replaced by nitrogen, and the reactor temperature was set at 273 K. The reduced catalysts were then put into a 1-butene/H_2 flow. The partial pressure of 1-butene was 50 Torr. The effluent gases were analyzed by the FID detector connected to a Plot Al_2O_3/KCl capillary column. The activity was calculated at the pseudostationary state after 2 h on stream. Conversion was kept below 10% by adjusting the weight of the catalyst or the total flow to avoid possible mass transfer limitation.

CO FTIR Spectroscopy

FTIR characterization of adsorbed CO was performed using self-supporting, pressed samples discs (10 mg for a disc diameter of 2 cm^2). Prior to the adsorption experiments, the catalysts were resulfided *in situ* in the infrared transmission cell. For this purpose, the pellet was first heated to 673 K under vacuum at a heating rate of 10 K min^{-1} and then put into contact with 100 Torr of H_2S (15%)He. The cell was kept at this temperature for 30 min. Sulfidation was followed by evacuation at 673 K for 30 min. This sulfidation–evacuation procedure was repeated twice before cooling the system down to room temperature under evacuation before solid reduction. Then, 200 Torr of pure hydrogen was introduced into the cell, which was heated to the T_r. Several reduction–evacuation cycles were conducted to remove the H_2S formed upon reduction. Finally, all the samples were evacuated at 393 K for 30 min prior to probe molecule adsorption. CO adsorption was then performed at low temperature (~100 K) using a specially designed IR cell. The hydrogen-treated catalysts were put into contact with either successive, small, and calibrated doses of CO or with 1 Torr of CO at equilibrium before evacuation at liquid nitrogen temperature or at room temperature. The IR spectra were recorded using a Nicolet 60SX FTIR spectrometer. Band intensities were corrected for slight differences in the weight of the catalyst and adjusted to 10 mg. The band areas were calculated by integration using IR Omnic software.

RESULTS

Solid Reduction and Physico–Chemical Characterization

The effect of hydrogen reduction on the silica-supported ruthenium sulf ide was studied in detail in a previous study (9). However, the main results will be summarized here to better understand our study about CO FTIR. As reported in Table 1, the degree of reduction increases with the reduction temperature, and at 673 K the catalyst is completely reduced in agreement with chemical analysis. HREM characterizations showed that the average particle size and the distribution width remained more or less the same up to $T_r = 573$ K. At higher T_r, sintering occurred and the distribution was considerably wider. Moreover, a metallic phase was detected by XRD. From these data, it is clear that the silica-supported ruthenium sulfide maintained its morphology up to 573 K, and when sintering occurred, the increase in the particle size was accompanied by the formation of a

TABLE 1

Degree of Reduction and Mean Particle Size after Hydrogen Treatment of RuS_2/SiO_2 at Various Reduction Temperatures (T_r) (Data in Italics (in Brackets) Correspond to the Standard Deviation of Particle Size Distribution)

Reduction temperature (K)	Degree of reduction (%)	Mean particle size (Å)
None	0	36 *(7)*
423	12	—
473	20	37 *(8)*
523	26	—
573	45	43 *(11)*
623	82	65 *(16)*
673	100	110 *(28)*

metallic phase. These results reflect the stability of silica-supported ruthenium sulfide, as was previously observed for the unsupported catalyst (6).

1-Butene Hydrogenation

Figure 1 shows the variation in the activity of butene hydrogenation as a function of the degree of reduction of the catalyst. The activity drastically increases upon solid reduction, reaches a maximum for $\alpha = \sim 40\%$, and then remains stable as the reduction treatment becomes more severe. This sequence of events differs from that observed for the CH_3SH condensation reaction (Ref. (9) and Fig. 1). The variation in the activity toward CH_3SH condensation is very similar to that reported for Lewis acidity, determined using pyridine as a probe molecule. This distinct catalytic reaction behaviour suggests that both reactions require different catalytic sites.

Infrared Spectroscopy of Adsorbed CO

Adsorption on the initial and nonreduced RuS_x/SiO_2. The variations in the IR spectra after the successive introduction of small amounts of CO are reported in Fig. 2. Bands appear in two main domains: 2100–2200 and 2000–2100 cm^{-1}. The high-frequency domain (HF: 2100–2200 cm^{-1}) presents two bands at 2157 and 2137 cm^{-1} and a shoulder at 2173 cm^{-1}. These bands are observed after 1.2 μmol of CO are introduced; their intensity increases as more CO is added, and they disappear upon evacuation at 100 K. In the low-frequency range (LF: 2000–2100 cm^{-1}), the spectrum exhibits two main bands at 2073 and 2035 cm^{-1} as well as a weak shoulder at $\sim$2092 cm^{-1}. These bands are detectable as soon as CO (0.09 μmol) is introduced; the frequency of the bands is not affected by larger amounts of CO or by the evacuation of the cell at low temperature (100 K), but the intensity of the bands increases upon evacuation. The distinct response to evacuation, as observed for the bands in the two delimited domains, indicates that the bands

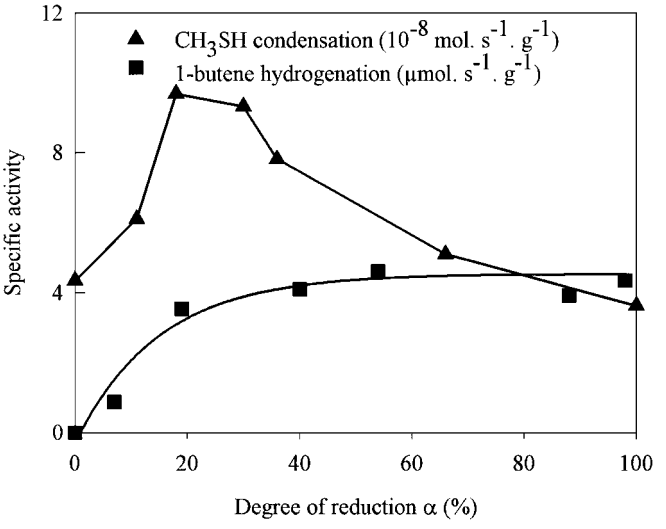

FIG. 1. Variation in the 1-butene hydrogenation and CH_3SH condensation activities as a function of the degree of reduction of the catalysts ($P_{H_2} = 710$ Torr; $P_{1\text{-Butene}} = 50$ Torr; $T = 273$ K; total flow = 50 cm^3/min; $P_{MeSH} = 40$ Torr in N_2; $T = 473$ K; total flow = 63 cm^3/min).

correspond to different species, depending on whether their wavenumber is high or low. Moreover, the high-frequency bands are also observed when CO is adsorbed on the support without a sulfided phase. Taking into account these results and literature data, the 2137-cm^{-1} band can be assigned to physisorbed CO species (23) and the 2157-cm^{-1} band to the interaction of CO with the hydroxyl groups of the silica support; the shoulder at 2173 cm^{-1} corresponds to the interaction of CO with the coordinatively unsaturated sites of alumina that are present as impurities in

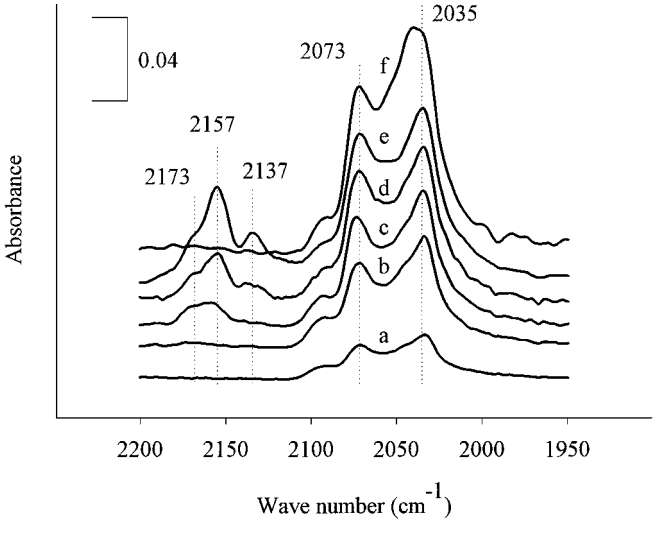

FIG. 2. IR spectra of CO species adsorbed on a nonreduced RuS_2/SiO_2 sample, after injection of (a) 0.09 μmol of CO, (b) 0.28 μmol, (c) 1.20 μmol, (d) 1 Torr at equilibrium pressure, (e) 5 Torr at equilibrium pressure, and (f) after evacuation at $\sim$100 K.

the support (20, 24, 25). The LF bands correspond to CO adsorption on Ru sites (26). The increase in the intensity of these bands after removal of the physisorbed CO species and the CO linked to the hydroxyl groups of the support may be due to a steric effect related to the presence of these weakly bounded CO species, thus limiting the accessibility of CO to the CUS sites of the Ru particles. This effect was already observed with low-temperature adsorption on metal-supported catalysts.

Adsorption on the silica-supported metallic Ru phase. To interpret these LF bands more fully, we compared CO adsorption on the completely reduced RuS_2/SiO_2 catalyst, formed by treating it at 773 K, and on metallic Ru, supported on silica and prepared by reducing the $RuCl_x/SiO_2$ catalyst precursor in an H_2 flow at 873 K (Fig. 3). The spectra obtained on both solids are close and exhibit a main band at 2035 ± 2 cm^{-1}, characteristic of Ru metal sites and in agreement with data reported in the literature (27–32). The 4-cm^{-1} shift (2033 cm^{-1} for the ex RuS_2/SiO_2; 2037 cm^{-1} for Ru/SiO_2) may be related to differences in the size of the particles. As well as this main adsorption band, the shoulder detected at 2016 cm^{-1} arises from the interaction of CO with metallic Ru sites with a low coordination number, located at the edges and/or corners of the particle (29). Moreover, an additional shoulder appears at 2056 cm^{-1} on totally reduced RuS_2/SiO_2, which is not detected on the nonsulfided precursor. Such a band was already observed by De Los Reyes *et al.* (26) on RuS_2/Al_2O_3. This may indicate that the 773 K hydrogen-treated RuS_2/SiO_2, which is mainly in a metallic phase, possesses a few surface Ru atoms that are still bound to some of the residual sulfur anions. According to these experimental observations, it is proposed that the concomitant appearance of bands at 2033–2037 and at 2016 cm^{-1} reveals the presence of a sulfur-depleted Ru site.

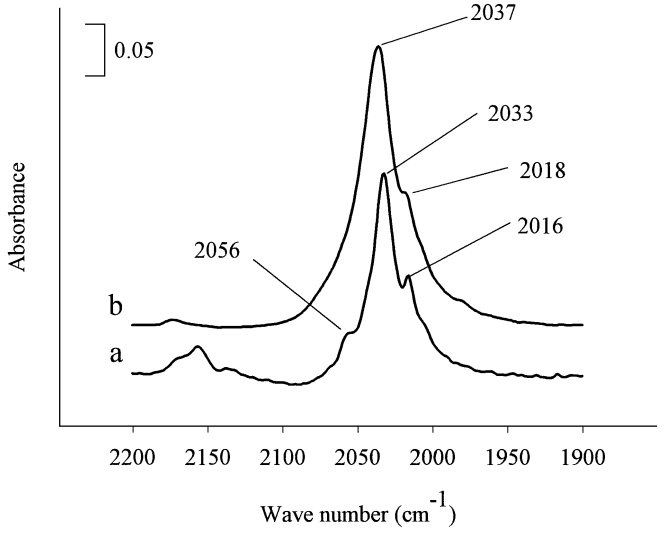

FIG. 3. Comparison of the IR spectra of CO species adsorbed on (a) a RuS_2/SiO_2 sample, totally reduced ($T_r = 773$ K) and (b) a $RuCl_x/SiO_2$ sample, nonsulfided and hydrogen-treated at 873 K (1 Torr CO at equilibrium pressure, $T = 100$ K).

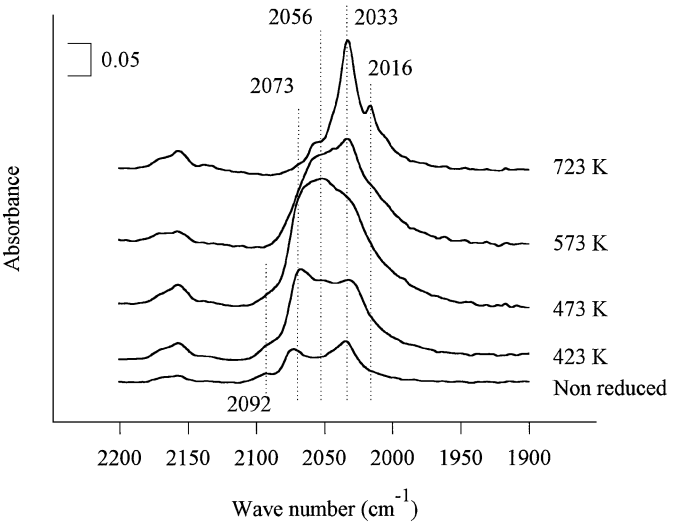

FIG. 4. Comparison of the IR spectra of CO species adsorbed on RuS_2/SiO_2 reduced at various temperatures (1 Torr CO at equilibrium pressure evacuated at ~100 K).

Influence of Progressive Reduction on the CO Adsorption Profiles

IR spectra of CO adsorbed on the RuS_2/SiO_2 catalyst that was reduced at various temperatures reveal several bands with wavenumbers from 2200 to 2000 cm^{-1} (Fig. 4). On the nonreduced sample, the main bands are detected at 2092, 2073, and 2033 cm^{-1} with a shoulder at ~2056 cm^{-1}. Upon reduction at 423 K, bands are detected at wavenumbers similar to those for a nonreduced sample but with higher intensities; the most intense absorption band was observed at 2073 cm^{-1}. If reduction is performed at $T_r = 473$ K, the optimum shifts from 2073 to 2056 cm^{-1} and then to 2033 cm^{-1} for $T_r \geq 573$ K. Meanwhile, the shoulder at 2092 cm^{-1} vanishes for $T_r \geq 573$ K, whereas the 2016-cm^{-1} signal is detected from $T_r = 573$ K ($\alpha = 45\%$). These results are evidence of an increase in the intensity of the bands and of a shift toward lower wavenumbers of the ν(CO) massif upon progressive reduction of the catalyst.

DISCUSSION

Infrared Spectroscopy

As reported previously, the ν(CO) vibrations located in the 2100- to 2000-cm^{-1} frequency range characterize chemical bonding of CO with the sorbing site of the sulfided phase. On the initial and nonreduced sample, four bands were observed at 2092, 2073, 2056, and 2033 cm^{-1}, despite

a high S/Ru ratio (∼2.7). This indicates that the initial solid already possesses some CUS, in agreement with previous data from pyridine and CH_3SH adsorption experiments (9, 10). All these bands remain upon slight reduction of the catalyst at either 423 or 473 K; only the relative intensity of the bands changes when sulfur is progressively removed from the solid; i.e., the band with the greater intensity is situated at 2033 cm^{-1} on the nonreduced sample, while the maxima is detected at 2073 cm^{-1} for a $T_r = 423$ K and then at 2056 cm^{-1} when the catalyst is reduced at 473 K. This change in the position of absorbance maxima in relation to catalyst reduction can be interpreted in terms of a modification of the electron density around the adsorbing site. According to the Blyholder model (11), the decrease in the number of electronegative species in the Ru cation environment enhances the ability of the metal to provide electrons from its *d* orbital to the $2\pi^*$ antibonding orbital of the CO probe (33). This back-donation reinforcement results in a ν(CO) shift toward lower wavenumbers. HREM results (Table 1) show that both the mean particle size and the change in the distribution remain the same up to $T_r = 573$ K. This indicates that the number of Ru cations present at the edges or at the corners of the particles is constant up to this temperature. Therefore, the shift of band maxima toward lower wavenumbers reflects a progressive decrease in the number of sulfur atoms in the first coordination shell of the cationic Ru site rather than a morphological modification of the solid upon reduction.

In this study, the simultaneous presence of several bands on a RuS_2/SiO_2 catalytic system denotes the concomitant existence of several kinds of Ru sites in various sulfur environments. Thus, we assumed that the bands at 2092, 2073, 2056, and 2033 cm^{-1} results from the interaction of CO with coordinatively unsaturated Ru sites having 1, 2, 3, or more sulfur vacancies, respectively. However, the detection of a band at 2033 cm^{-1}, both on the nonreduced sample and on the completely reduced Ru catalyst, is surprising (Figs. 3 and 4). For the nonreduced solid, this band may not be due to pure metallic sites since the initial S/Ru ratio corresponds to an overstoichiometric composition (S/Ru = 2.7). Literature data (20, 33) point out that CO adsorption on a supported Ru catalyst leads to complex spectra involving various CO species. There is general agreement as to attributing the low-frequency band at 2050–2030 cm^{-1} to CO linear adsorption on a Ru^0 reduced site. However, some papers provided evidence of the presence of $Ru^{n+}(CO)_2$ compounds characterized by a pair of bands at 2100–2057 cm^{-1} and 2038–1970 cm^{-1} (17, 34–40). Therefore, the formation of such species could occur on the sulfided phase. The band at 2033 cm^{-1} may be the low-frequency component of these dicarbonyl species. Therefore, at low degrees of reduction, the simultaneous presence of both bands at 2073 and 2035 cm^{-1} (Fig. 2) may be related to the dicarbonyl species adsorbed on the sulfided phase. In contrast, the appearance for $T_r \geq 573$ K of the shoulder at 2016 cm^{-1} confirms the formation of a metallic particle because this band is not observed on the nonreduced sample. Consequently, the 2033-cm^{-1} band characterizes the presence of dicarbonyl species fixed on CUS of the sulfided phase or the presence of monocarbonyl species adsorbed on the Ru metallic phase. Therefore, the simultaneous presence of the band at 2033 cm^{-1} and of the shoulder at 2016 cm^{-1} on the catalyst reduced at 573 K suggests the formation of some metallic Ru microdomains.

The integrated areas of the more pronounced IR bands were determined as related to the degree of reduction. The ν(CO) massif was then decomposed into five components using the commercial Peakfit software. The wavenumbers, the shape, and the FWMH parameters of each band were kept constant at the various reduction temperatures. The data calculated by means of this procedure are given in Fig. 5. These results correspond to relative variations in the number of sites since the molar extinction coefficient of these bands probably varies. The intensity of the 2092-cm^{-1} component remains very weak and was not detected until the degree of reduction (α) attained 45%. The 2056- and 2073-cm^{-1} signals increased rapidly from the beginning of the reduction, reached a maximum at $\alpha = 20\%$, and then decreased. Similar evolution of the intensity of these bands with α confirms that they arise from the interaction of CO with sites of the same nature. In contrast, the intensity of the 2033-cm^{-1} band increased with α, reached a maximum for $\alpha = 45\%$, and then decreased slightly with higher T_r. The discrepancy between the variations in the 2073- and 2033-cm^{-1} bands is in agreement with the dual assignment of the latter band to the sulfide and metallic phases. The increase in the 2073- and 2033-cm^{-1} signal up

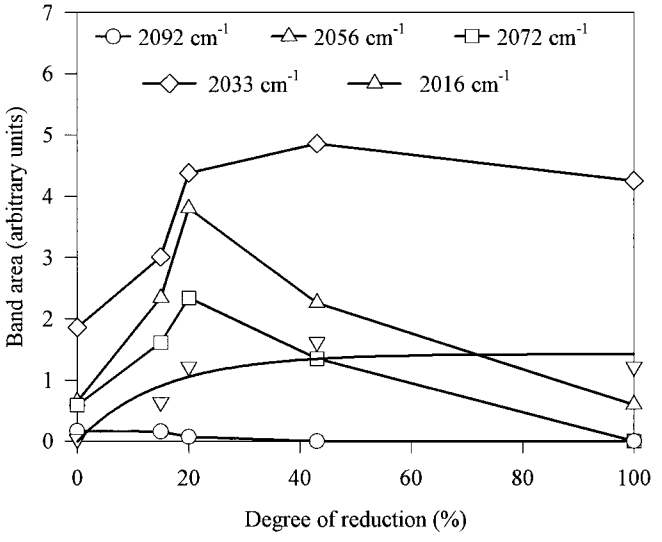

FIG. 5. Variation in the ν(CO) band areas versus the degree of reduction of RuS_2/SiO_2.

to 473 K ($\alpha = 20\%$) shows that the band intensity ratio is constant, as expected from the attribution of these bands to dicarbonyl species. For $473 < T_r < 573$ K ($20 < \alpha < 45\%$), the 2073-cm^{-1} band decreases rapidly, while the intensity of the 2033-cm^{-1} band remains relatively constant. This corresponds to the transformation of the sulfide into the metallic phase. In this case, the assignment of the 2033-cm^{-1} band to metallic sites is confirmed by the presence of the shoulder at 2016 cm^{-1}. The 2033-cm^{-1} band has the same intensity, even at higher degrees of reduction, suggesting that the increase in the amount of the metallic phase compensates the sintering which appears for the high T_r. In addition to these four bands, the evolution of a 2016-cm^{-1} band has been reported; its presence is not necessary to properly fit the spectrum of the nonreduced catalyst. Its intensity then increases exponentially and also stabilizes for $\alpha \sim 45\%$.

To sum up, the 2093-cm^{-1} signal results from linear adsorption on Ru CUS in a very sulfided environment. The 2056-cm^{-1} band and the pair of bands at 2073 with a fraction of the band at 2033 cm^{-1}, respectively characterizes mono- and dicarbonyl species adsorbed on Ru cations that have a lower coordination in sulfur atoms. The simultaneous presence of the band at 2033 cm^{-1} and the shoulder at 2016 cm^{-1} indicates the formation of a metallic Ru phase. Consequently, the reductive treatment involves a heterogeneous desulfurization process since the sulfided and metallic phases coexist, particularly for degrees of reduction around 40–50%. At intermediate reduction temperatures, the metallic phase is obviously present as very small domains because it was not detected by XRD (9).

Correlation Infrared Spectroscopy—Catalytic Activities

Data reported in Fig. 1 clearly show that the reaction of 1-butene hydrogenation and the CH_3SH condensation reaction do not require the same type of sites. Indeed, the CH_3SH condensation presents a maximum activity for $\alpha = 20\%$, while hydrogenation activity increases and reaches a plateau for $\alpha = 45\%$. Since this work demonstrates the existence of several types of Ru sites, differing in their sulfur environment and the number of which varies with reduction temperatures (Fig. 5), a comparison between the variation in these sites and the activity for these two test reactions was carried out.

Previous work shows that variations in both the CH_3SH activity and in the amount of adsorbed pyridine or CH_3SH with the degree of reduction (α) of the catalyst follow the same trend. These results lead to the conclusion that this reaction requires a coordinatively unsaturated Ru site and a neighboring anionic sulfur species, on which the reactant dissociates and leads to a thiolate and an SH species. The present work on CO adsorption reveals that the activity in this reaction requiring acidic sites follows the same trend as the 2073- and 2056-cm^{-1} ν(CO) band areas (Fig. 6). Consequently, it confirms that these bands are characteristic of CUS in a sulfided environment with Lewis acid-type properties. For $20 < \alpha < 45\%$, a similar decrease in the CH_3SH activity (as well as the pyridine adsorption) and in these band intensities reflects a diminution in the acidic character of the catalyst. This indicates that a sulfur-rich environment around the Ru sites must be maintained to confer Lewis acidity to the RuS_2/SiO_2 system. In this range, metallic microdomains are proven by the concomitant appearance of the ν(CO) bands at 2033 and 2016 cm^{-1}, as long as the reduction of the catalyst proceeds gradually. These microdomains are probably the intermediate nuclei required in the formation of the metallic particles detected by XRD and HREM at $T_r = 573$ K ($\alpha = 45\%$). If these sites are not involved in pyridine chemisorption properties, then conversely they play a direct and important role in hydrogenation since the

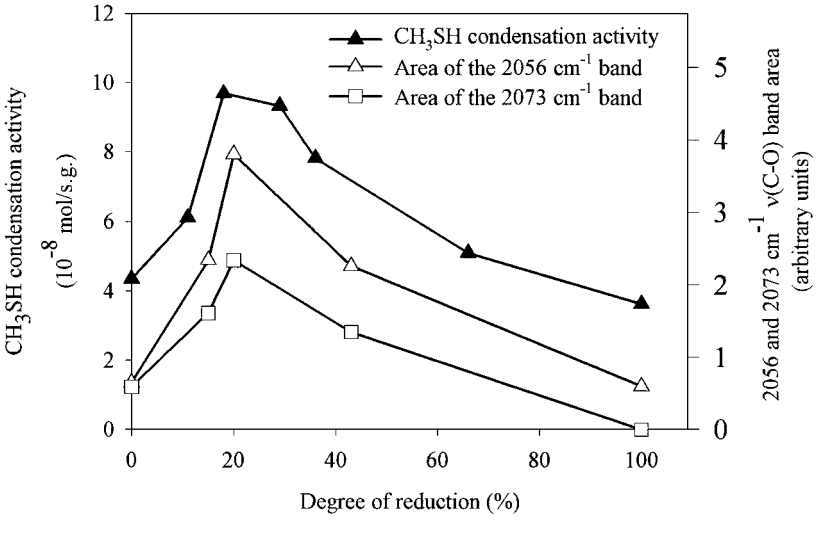

FIG. 6. A comparison of variations in the CH_3SH condensation activity and in the 2056- and 2073-cm^{-1} ν(C-O) band areas on RuS_2/SiO_2 versus the degree of reduction.

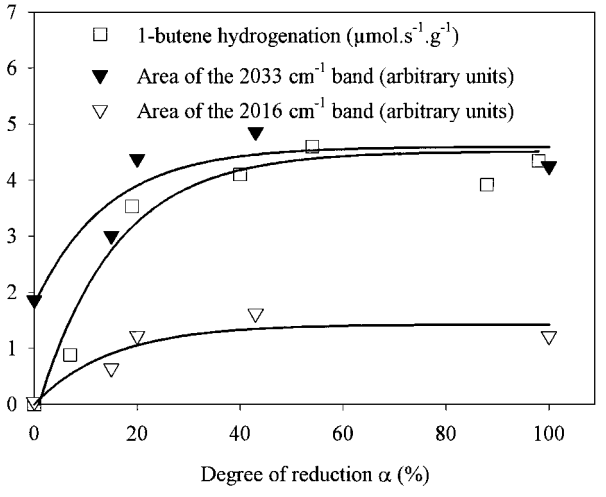

FIG. 7. A comparison of the variations in 1-butene hydrogenation activity and in the 2033- and 2016-cm^{-1} ν(C-O) band areas versus the degree of reduction of RuS_2/SiO_2.

evolution with α of both the 1-butene activity and the intensity of the ν(CO) at 2016 cm^{-1} follows the same trend (Fig. 7). This shows that the properties of the RuS_2 phase moved progressively from an acidic state to a metallic state.

CONCLUSION

The interaction of hydrogen with the RuS_2 phase modifies the S/Ru ratio to a large extent (up to 45% of sulfur removal) without changing the structure and morphology of the Ru particles. In this stability range, the progressive reduction of the surface induces a change in the number of CUS and SH groups. CO adsorption measurements demonstrated a continuous modification of these surface properties with the simultaneous presence of Ru sites in different coordination states, which coexist with microdomains of the metallic phase. This progressive transition of the electronic properties strongly affects the catalytic properties of the solid. A sulfur-rich environment is required to obtain significant activities in reactions requiring acid, such as the transformation of CH_3SH to CH_3SCH_3, while 1-butene hydrogenation requires sulfur-depleted sites to proceed. Consequently, the catalysts gradually move from acidic properties to metallic properties when sulfur is removed from the surface.

ACKNOWLEDGMENTS

This work was carried out within the scope of a scientific program of collaboration between France and China. G. Berhault is greatly indebted to the French Ministry of Education for a Ph.D. grant.

REFERENCES

1. Tanaka, K., *Adv. Catal.* **33**, 99 (1985).
2. Wambeke, A., Jalowiecki, L., Kasztelan, S., Grimblot, J., and Bonnelle, J. P., *J. Catal.* **109**, 320 (1988).
3. Joffre, J., Geneste, P., and Lerner, D. A., *J. Catal.* **97**, 543 (1986).
4. Diez, R. P., and Jubert, A. H., *J. Mol. Catal.* **83**, 219 (1993).
5. Kasztelan, S., Wambeke, A., Jalowiecki, L., Grimblot, J., and Bonnelle, J. P., *J. Catal.* **124**, 543 (1990).
6. Lacroix, M., Yuan, S., Breysse, M., Dorémieux-Morin, C., and Fraissard, J., *J. Catal.* **138**, 409 (1992).
7. Lacroix, M., Mirodatos, C., Breysse, M., Décamp, T., and Yuan, S., *in* "New Frontiers in Catalysis" (L. Guczi, F. Solymosi, and P. Tétényi, Eds.), p. 597. Elsevier, Budapest, 1993.
8. Yuan, S., Decamp, T., Lacroix, M., Mirodatos, C., and Breysse, M., *J. Catal.* **132**, 253 (1991).
9. Berhault, G., Lacroix, M., Breysse, M., Maugé, F., Lavalley, J.-C., and Qu, L. L., *J. Catal.* **170**, 37 (1997).
10. Berhault, G., Lacroix, M., Breysse, M., Maugé, F., Lavalley, J.-C., Nie, H., and Qu, L. L., *J. Catal.* **178**, 555 (1998).
11. Blyholder, G. J., *J. Phys. Chem.* **79**, 756 (1975).
12. Davydov, A. A., "Infrared Spectroscopy of Adsorbed Species on the Surface of Transition Metal Oxides" (C. H. Rochester, Ed.). Wiley, New York, 1990.
13. Little, L., "Infrared Spectra of Adsorbed Species." Academic Press, London/New York, 1966.
14. Busca, G., *Catal. Today* **41**, 191 (1998).
15. Yokomizo, G. H., Louis, C., and Bell, A. T., *J. Catal.* **120**, 1 (1989).
16. Solymosi, F., and Rasko, J., *J. Catal.* **115**, 120 (1989).
17. Zanderighi, G. M., Dossi, C., Ugo, R., Psaro, R., Theolier, A., Choplin, A., D'Ornelas, L., and Basset, J. M., *J. Organomet. Chem.* **296**, 127 (1985).
18. Mizushima, T., Tohji, K., Udagawa, Y., and Uneo, A., *J. Phys. Chem.* **94**, 4980 (1990).
19. Mizushima, T., Tohji, K., Udagawa, Y., and Uneo, A., *J. Am. Chem. Soc.* **112**, 7887 (1990).
20. Hadjiivanov, K., Lavalley, J.-C., Lamotte, J., Maugé, F., Saint-Just, J., and Che, M., *J. Catal.* **176**, 415 (1998).
21. Hadjiivanov, K., and Klissurski, D., *Chem. Soc. Rev.* **25**, 61 (1996).
22. Knop, O., *Can. J. Chem.* **41**, 1838 (1963).
23. Zaki, M. I., and Knözinger, H., *Mater. Chem. Phys.* **17**, 201 (1987).
24. Ballinger, T. H., and Yates, J. T., *Langmuir* **7**, 3041 (1991).
25. Parker, S. F., Amorelli, A., Amos, Y. D., Hughes, C., Porter, N., and Walton, J., *J. Chem. Soc., Faraday Trans.* **91**, 517 (1995).
26. De Los Reyes, J. A., Vrinat, M., Breysse, M., Maugé, F., and Lavalley, J.-C., *Catal. Lett.* **13**, 213 (1992).
27. Guglielminotti, E., and Bond, G. C., *J. Chem. Soc., Faraday Trans.* **86**, 979 (1990).
28. Solymosi, F., Erdöhelyi, A., and Kocsis, M., *J. Chem. Soc., Faraday Trans. 1* **77**, 1003 (1981).
29. Davydov, A. A., and Bell, A. T., *J. Catal.* **49**, 332 (1977).
30. Kostov, K., Rauscher, H., and Menzel, D., *Surf. Sci.* **278**, 62 (1992).
31. Hoffmann, F. M., and Weisel, M. D., *Surf. Sci.* **269/270**, 495 (1992).
32. Kevin Kuhn, W., He, J. W., and Goodman, D. W., *J. Vac. Sci. Technol.* **101**, 2477 (1992).
33. Sheppard, N., and Nguyen, T. T., *Adv. Infrared Raman Spectrosc.* **5**, 67 (1978).
34. D'Ornelas, L., Theolier, A., Choplin, A., and Basset, J., *Inorg. Chem.* **27**, 1261 (1988).
35. Burkhardt, I., Gudtschick, D., Landmesser, H., and Miessner, H., *in* "Zeolite Chemistry and Catalysis" (P. A. Jacobs *et al.*, Eds.), p. 215. Elsevier, Amsterdam, 1991.
36. Knözinger, H., Zhao, Y., Tesche, B., Barth, R., Epstein, R., Gates, B. C., and Scott, J. P., *Faraday Discuss. Chem. Soc.* **72**, 53 (1985).
37. Beck, A., Dobos, S., and Guczi, L., *Inorg. Chem.* **27**, 3220 (1988).
38. Uchiyama, S., and Gates, B. C., *J. Catal.* **110**, 388 (1988).
39. Evans, J., and McNulty, G. S., *J. Chem. Soc., Dalton Trans.* **80**, 1123 (1984).
40. Landmesser, H., and Miessner, H., *J. Phys. Chem.* **95**, 10544 (1991).